Journal of Inorganic Biochemistry xxx (2013) xxx–xxx

Contents lists available at SciVerse ScienceDirect

Journal of Inorganic Biochemistry

journal homepage: www.elsevier.com/locate/jinorgbio

Oxidovanadium(IV) and dioxidovanadium(V) complexes of tridentate salicylaldehyde semicarbazones: Searching for prospective antitrypanosomal agents

Mariana Fernández [a], Lorena Becco [b], Isabel Correia [c], Julio Benítez [a], Oscar E. Piro [d], Gustavo A. Echeverria [d], Andrea Medeiros [e,f], Marcelo Comini [f], María Laura Lavaggi [g], Mercedes González [g], Hugo Cerecetto [g], Virtudes Moreno [h], Joao Costa Pessoa [c], Beatriz Garat [b], Dinorah Gambino [a,*]

[a] Cátedra de Química Inorgánica, Facultad de Química, UDELAR, Gral. Flores 2124, 11800 Montevideo, Uruguay
[b] Laboratorio de Interacciones Moleculares, Facultad de Ciencias, UDELAR, Iguá 4225, 11400 Montevideo, Uruguay
[c] Centro de Química Estrutural, Instituto Superior Técnico, Universidade Técnica de Lisboa, Av Rovisco Pais, 1049-001 Lisboa, Portugal
[d] Departamento de Física, Facultad de Ciencias Exactas, Universidad Nacional de La Plata and IFLP (CONICET, CCT-La Plata), C.C. 67, 1900 La Plata, Argentina
[e] Departamento de Bioquímica, Facultad de Medicina, Universidad de la República, Montevideo, Uruguay
[f] Group Redox Biology of Trypanosomes, Institut Pasteur de Montevideo, Mataojo 2020, CP 11400, Montevideo, Uruguay
[g] Grupo de Química Medicinal, Laboratorio de Química Orgánica, Facultad de Ciencias-Facultad de Química, Universidad de la República, Iguá 4225, Montevideo 11400, Uruguay
[h] Departamento de Química Inorgánica, Universitat Barcelona, Martí i Franquès 1-11, 08028 Barcelona, Spain

ARTICLE INFO

Article history:
Received 10 December 2012
Received in revised form 20 February 2013
Accepted 20 February 2013
Available online xxxx

Keywords:
Oxidovanadium(IV) complexes
Dioxidovanadium(V) complexes
Salicylaldehyde semicarbazones
Antitrypanosomal
2,2′-bipyridine, dipyrido[3,2-a: 2′,3′-c] phenazine

ABSTRACT

As a contribution to the identification of the relevant species for biological activity and the understanding of structure–activity relationships of [$V^{IV}O$(L-2H)(NN)] antitrypanosomal complexes (NN is a bidentate polypyridyl DNA intercalator; L is a tridentate salicylaldehyde semicarbazone derivative), new [$V^{V}O_2$(L-2H)] complexes and [$V^{IV}O$(L-2H)(NN)] complexes including bipy or dppz (dipyrido[3,2-a: 2′,3′-c]phenazine) co-ligands are prepared and characterized in the solid state and in solution. Their activity is evaluated on *Trypanosoma cruzi*. The lipophilicity, as structural descriptor related to bioactivity, of the whole [$V^{IV}O$(L-2H)(NN)] series is determined. Furthermore, the antiproliferative effect of those new compounds showing activity against *T. cruzi* is evaluated on the genetically related parasite *T. brucei* with the aim to develop broad spectrum agents. The new [$V^{IV}O$(L-2H)(dppz)] complexes are about ten to fifteen times more toxic to *T. cruzi* than the bipy analogues and show quite good in vitro activity on *T. brucei brucei*. They are shown to interact with DNA, suggesting that this biomolecule may be the parasite target. The stability of the $V^{IV}O$-complexes in solution is accessed by several techniques. Globally the data suggest that the relevant species for biological activity are the [$V^{IV}O$(L-2H)(NN)] compounds, their order of activity being dependent on the NN nature, but not much on the substitution on the salicylaldehyde semicarbazone moiety. A parabolic relationship between biological response and lipophilicity (determined as $R_M = \log [(1 / R_f) - 1]$ by a TLC method) is obtained. From this correlation an optimum R_M value, close to 1.44, was found, which may be used as design guide for future development of antitrypanosomal compounds.
© 2013 Elsevier Inc. All rights reserved.

1. Introduction

The possible physiological roles of vanadium in biological systems and its pharmacological activities have led to a considerable amount of research. Efforts developing the medicinal chemistry of vanadium have mainly focused whether on improving biodistribution and tolerability of the vanadium insulin-enhancing core or on developing potential anti-tumor compounds [1–9]. Despite the fact that parasitic diseases are among the most prevalent illnesses worldwide, work on vanadium compounds for the potential treatment of some of these diseases has only arisen in recent years [10,11].

Inorganic medicinal chemists have demonstrated that the development of bioactive metal-based compounds could be a promising approach in the search for new drugs against some parasitic diseases [10,12–19]. In particular, pioneering research by Sánchez-Delgado, Biot and Brocard led to the identification of some interesting potential metallopharmaceuticals for Chagas disease and malaria [13,20–24].

Among the top neglected diseases are American trypanosomiasis (Chagas disease), human African trypanosomiasis (sleeping sickness) and Leishmaniasis. They are caused by genetically related single-celled protozoa parasites that belong to the family Trypanosomatidae. In particular, American trypanosomiasis and human African trypanosomiasis constitute major health concerns in the poorest tropical and subtropical regions of the world [25–28]. The trypanosomiasis and leishmaniasis are among the ten most prevalent diseases caused by protozoan parasites.

American trypanosomiasis (etiologic agent: *Trypanosoma cruzi*) is endemic of Latin America where it affects around 10 million people and causes more deaths in this region than any other parasitic disease. Globalization and immigration has also led to the appearance of several

* Corresponding author. Tel.: +598 29249739; fax: +598 29241906.
E-mail address: dgambino@fq.edu.uy (D. Gambino).

0162-0134/$ – see front matter © 2013 Elsevier Inc. All rights reserved.
http://dx.doi.org/10.1016/j.jinorgbio.2013.02.010

ARTICLE IN PRESS

infection cases in developed countries [26,29]. Sleeping sickness, which is caused by parasites from the *Trypanosoma brucei* complex (e.g. *Trypanosoma brucei gambiense* and *Trypanosoma brucei rhodesiense*), represents a major disease burden in sub-Saharian regions of Africa. Most of the available treatments against both diseases are based on decades-old non-specific drugs that give rise to undesirable collateral toxic effects, show limited and variable efficacy depending on the type or stage of the disease and suffer from parasite's development of resistance. Therefore, the development of more efficacious and less toxic drugs, that could also circumvent emerging drug resistance, is urgently needed [25,27,29–31].

Several attempts to develop anti-parasitic metal-based drugs are currently in progress through distinct approaches. Although our group has been mainly devoted to the search for new metal-based antitrypanosomatid drugs through metal complexation of anti-parasitic organic compounds in an attempt to modulate their activity [10,18,19], more recently we also began exploring another strategy which consists in binding to DNA metal complexes containing ligands with intercalating capacity, thus placing this biomolecule as the target in the parasite [10]. Molecules able to irreversibly modify nucleic acids have received considerable attention due to their prospective applications in drug design. This strategy is based on the observation that highly-proliferative cells such as *Trypanosoma* parasites and tumor cells show metabolic similarities that lead in many cases to a correlation between antitrypanosomal and antitumor activities. For instance, some compounds that efficiently interact with DNA in an intercalative mode have been shown to exert antileishmanial and/or antitrypanosomal activity [10,12,13,19,32]. Our research following this strategy led to the development of $[V^{IV}O(SO_4)(H_2O)_2(dppz)]\cdot 2H_2O$ and a series of mixed-ligand oxidovanadium(IV) complexes, $[V^{IV}O(L\text{-}2H)(NN)]$, including as ligands: (i) a bidentate polypyridyl DNA intercalator, abbreviated as NN (NN = dppz = dipyrido[3,2-a: 2′,3′-c]phenazine, bipy = 2,2′-bipyridine, phen = 1,10-phenanthroline), and (ii) a tridentate salicylaldehyde semicarbazone derivative (L). These complexes displayed IC_{50} values in the micromolar range against *T. cruzi* (Dm28c strain, epimastigote form of the parasite life cycle), in most of the cases were slightly more active (in a molar basis) than the reference trypanosomicidal drug Nifurtimox, and showed to interact with DNA, hence suggesting that this biomolecule may be the parasite target [33–35].

As a contribution to the understanding of structure-activity relationships in the above mentioned systems, in this work we further address a similar type of mixed-ligand complexes by synthesizing six new $[V^{IV}O(L\text{-}2H)(NN)]$ complexes, hereafter named compounds **4–9**, with L = L3–L5 and NN = bipy or dppz (Fig. 1). The complexes were characterized in the solid state and in solution by several techniques, and their biological activity was evaluated on *T. cruzi*. The lipophilicity of the compounds was determined and then correlated with the observed activity in order to perform a preliminar QSAR (quantitative structure–activity relationship) study. Furthermore, the antiproliferative effect of those new compounds showing activity against *T. cruzi* was evaluated on the genetically related parasite *T. brucei* with the aim to evaluate the approach of developing new broad spectrum antitrypanosomal agents based on the presence of common targets in both parasites.

Previous EPR and ^{51}V NMR studies carried out in solvents having moderate coordinating ability towards metal ions (DMSO or DMF (dimethylformamide)) suggested that the complexes could undergo hydrolysis, oxidation and release of the NN ligand in solution, leading to dioxidovanadium(V) semicarbazone complexes that could be responsible for the bioactivity [34,35]. Nevertheless, the antitrypanosomal activity of the previously developed $[V^{IV}O(L\text{-}2H)(NN)]$ series showed a clear correlation with the nature of the NN ligand and not with the substitution on the salicylaldehyde semicarbazone moiety [34,35]. Therefore, in the current work three new $V^{V}O_2$-semicarbazone complexes $[V^{V}O_2(L\text{-}H)]$ with L = L3–L5, compounds **1–3**, were synthesized, characterized and evaluated against *T. cruzi* together with the previously reported analogous $V^{V}O_2$-compounds of L1 and L2 [36–38].

2. Materials and methods

2.1. Materials

All common laboratory chemicals were purchased from commercial sources and used without further purification. Semicarbazone ligands were synthesized from an equimolar mixture of the corresponding aldehyde and semicarbazide and characterized by C, H and N elemental analyses, and by FTIR and ^{1}H and ^{13}C NMR spectroscopies [34–39]. $[V^{V}O_2(L\text{-}H)]$ complexes, where L = salicylaldehyde semicarbazone (L1) or 5-bromosalicylaldehyde semicarbazone (L2) were also synthesized

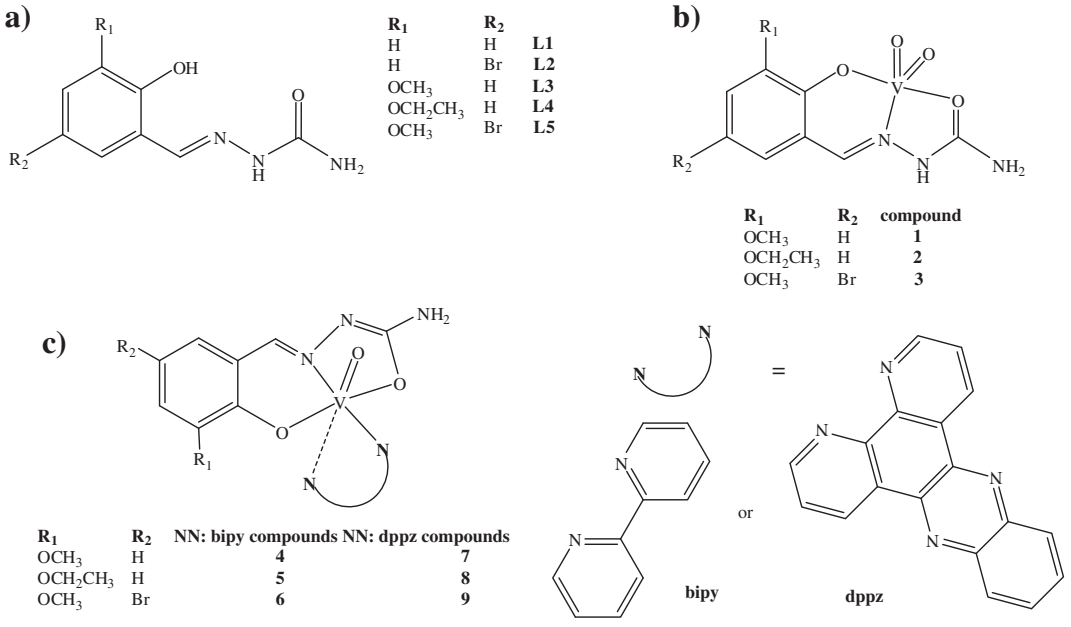

Fig. 1. a) Salicylaldehyde semicarbazone derivatives L selected as ligands (L1–L5); b) new $[V^{V}O_2(L\text{-}H)]$ complexes **1–3**; c) new $[V^{IV}O(L\text{-}2H)(NN)]$ complexes, where NN = bipy (**4–6**) or dppz (**7–9**).

Please cite this article as: M. Fernández, et al., Oxidovanadium(IV) and dioxidovanadium(V) complexes of tridentate salicylaldehyde semicarbazones: Searching for prospective antitry..., J. Inorg. Biochem. (2013), http://dx.doi.org/10.1016/j.jinorgbio.2013.02.010

and characterized as previously described [36–38]. Previously reported complexes, namely $V^{IV}O$(L-2H)(NN) with NN = bipy, dppz or phen, were also synthesized and characterized as described in the literature [34,35].

2.2. Syntheses of the dioxidovanadium(V) complexes, [$V^{V}O_2$(L-H)], 1–3

The new [$V^{V}O_2$(L-H)] complexes, where L = 2-hydroxy-3-methoxybenzaldehyde semicarbazone (L3), 3-ethoxysalicylaldehyde semicarbazone (L4) or 5-bromo-2-hydroxy-3-methoxybenzaldehyde semicarbazone (L5), were prepared by first mixing [$V^{IV}O(acac)_2$] (100 mg, 0.375 mmol, acac = acetylacetonate) with L (0.375 mmol) in ethanol (10 mL) and then keeping for 24 h under reflux. The reaction mixture was then stirred during 5–10 days at room temperature. In each case a yellow solid was isolated by centrifugation and recrystallized from boiling ethanol.

[$V^{V}O_2$(L3-H)], 1. Yield: 42 mg, 39%. Anal (%) calc. for $C_9H_{10}N_3O_5V$: C, 37.2; H, 3.4; N, 14.4. Found: C, 37.6; H, 3.4, N, 14.1. Λ_M(DMF): 5.0 μS/cm^2

[$V^{V}O_2$(L4-H)], 2. Yield: 94 mg, 82%. Anal (%) calc. for $C_{10}H_{12}N_3O_5V$: C, 39.4; H, 4.0; N, 13.8. Found: C, 39.6; H, 4.3; N, 13.7. Λ_M(DMF): 7.0 μS/cm^2

[$V^{V}O_2$(L5-H)]·H_2O, 3. Yield: 61 mg, 44%. Anal (%) calc. for $C_9H_{11}BrN_3O_6V$: C, 27.9; H, 2.9; N, 10.4. Found: C, 27.8; H, 2.9; N, 10.3. Λ_M(DMF): 6.0 μS/cm^2

2.3. Syntheses of the oxidovanadium(IV) complexes, [$V^{IV}O$(L-2H))NN], NN = bipy, 4–6, or dppz, 7–9

The new [$V^{IV}O$(L-2H)(NN)] complexes, where L = L3–L5 and NN = bipy or dppz, were synthesized by the following procedure: 0.375 mmol of L (78 mg L3, 84 mg L4 or 108 mg L5) and 0.375 mmol of NN (59 mg bipy or 110 mg dppz) were suspended in 15 mL of absolute alcohol previously purged with nitrogen for 10 min. [$V^{IV}O(acac)_2$] (0.375 mmol, 100 mg) was suspended in 6 mL of absolute alcohol, previously purged with nitrogen, and was added to the previous mixture. This was then heated at reflux under nitrogen for 3.5 h. The brown-red solid formed was filtered off from the hot mixture, and then washed three times with 2 mL portions of EtOH:Et_2O (1:1).

[$V^{IV}O$(L3-2H)(bipy)]·$2H_2O$, 4. Yield: 48 mg, 27%. Anal. calc. for $C_{19}H_{21}N_5O_6V$: C, 48.9; H, 4.5; N, 15.0. Found: C, 48.7; H, 4.0; N, 14.9. ESI-MS (electrospray ionization mass spectra) (MeOH) *m/z* [Found (Calcd)]: 431.1 (431.1) (55%) (M + H^+). Λ_M(DMF): 8.0 μS/cm^2.

[$V^{IV}O$(L4-2H)(bipy)]·H_2O, 5. Yield: 80 mg, 46%. Anal. calc. for $C_{20}H_{21}N_5O_5V$: C, 51.9; H, 4.6; N, 15.1. Found: C, 51.7; H, 4.6; N, 14.8. ESI-MS (MeOH) *m/z* [Found (Calcd)]: 445.2 (445.1) (100%) (M + H^+). Λ_M(DMF): 9.1 μS/cm^2.

[$V^{IV}O$(L5-2H)(bipy)].H_2O, 6. Yield: 97 mg, 49%. Anal. calc. for $C_{19}H_{18}BrN_5O_5V$: C, 43.3; H, 3.4; N, 13.3. Found: C, 43.2; H, 3.1; N, 13.2. ESI-MS (MeOH) *m/z* [Found (Calcd)]: 509.1 (509.0) (100%) (M + H^+) (Br isotope pattern found as expected). Λ_M(DMF): 8.0 μS/cm^2.

[$V^{IV}O$(L3-2H)(dppz)], 7. Yield: 88 mg, 42%. Anal. calc. for $C_{27}H_{19}N_7O_4V$: C, 58.3; H, 3.4; N, 17.6. Found: C, 58.2; H, 3.3; N, 17.4. ESI-MS (MeOH) *m/z* [Found (Calcd)]: 282.9 (283.1) (10%) (Hdppz$^+$), 556.7 (556.09) (25%) (M + H^+). Λ_M(DMF): 7.5 μS/cm^2.

[$V^{IV}O$(L4-2H)(dppz)], 8. Yield: 160 mg, 75%. Anal. calc. for $C_{28}H_{21}N_7O_4V$: C, 59.0; H, 3.7; N, 17.2. Found: C, 58.8; H, 3.6; N, 17.1. ESI-MS (MeOH) *m/z* [Found (Calcd)]: 282.9 (283.1) (45%) (Hdppz$^+$), 570.7 (571.1) (90%) (M + H^+). Λ_M(DMF): 6.6 μS/cm^2.

[$V^{IV}O$(L5-2H)(dppz)], 9. Yield: 176 mg, 74%. Anal. calc. for $C_{27}H_{18}BrN_7O_4V$: C, 51.0; H, 2.9; N, 15.4. Found: C, 50.8; H, 2.9; N, 15.5. ESI-MS (MeOH) *m/z* [Found (Calcd)]: 282.9 (283.1) (50%) (Hdppz$^+$), 634.6 (635.01) (25%) (M + H^+) (Br isotope pattern found as expected). Λ_M(DMF): 7.8 μS/cm^2.

2.4. Physicochemical characterization

C, H and N analyses were carried out with a Carlo Erba Model EA1108 elemental analyzer. Thermogravimetric measurements were done with a Shimadzu TGA 50 thermobalance, with a platinum cell, working under flowing nitrogen (50 mL/min) and at a heating rate of 0.5 °C/min (RT-80 °C) and 1.0 °C/min (80–350 °C). Conductimetric measurements were done at 25 °C in 10^{-3} M DMF solutions using a Conductivity Meter 4310 Jenway [40]. Conductivity measurements of DMSO-H_2O solutions were also done over time in order to access the stability of the complexes in such medium. A 500-MS Varian Ion Trap Mass Spectrometer was used to measure ESI-MS of methanolic solutions of the complexes in the positive mode (after dissolution of the complexes in a very small amount of DMF). A combination of several scans was made for each sample.

The FTIR absorption spectra (4000–400 cm^{-1}) of the complexes and the free ligands were measured as KBr pellets with a Bomen FTIR model M102 instrument. ^{1}H NMR spectra of the free ligands and of the $V^{V}O_2$-complexes in DMSO-d_6 were recorded at 30 °C on a Bruker DPX-400 instrument (at 400 MHz). Heteronuclear correlation experiments (2D-HETCOR), HMQC (heteronuclear multiple quantum correlation) and HMBC (heteronuclear multiple bond correlation), were carried out with the same instrument. The UV–vis absorption spectra were measured with a Perkin Elmer Lambda 35 spectrophotometer. ^{51}V NMR spectra of ca. 3 mM solutions of the complexes in DMF (p.a. grade) (5–10% D_2O was added) were recorded on a Bruker Avance III 400 MHz instrument. ^{51}V chemical shifts were referenced relative to neat $VOCl_3$ as external standard. EPR spectra were recorded either at 77 K or at 100 K with a Bruker ESP 300E X-band spectrometer coupled to a Bruker ER041 X-band frequency meter (9.45 GHz). Complexes were dissolved at room temperature in DMF p.a. grade (3 mM), previously degassed by passing N_2 for 10 min, and the solutions were immediately frozen in liquid nitrogen. The spin Hamiltonian parameters were obtained by simulation of the spectra with the computer program of Rockenbauer and Korecz [41] or by an iterative procedure using equations proposed by Chasteen [42] and corrected by Casella [43].

2.5. Crystallographic study

Suitable crystals for structural single crystal X-ray diffraction studies of [$V^{V}O_2$(L3-H)]·CH_3CH_2OH were obtained by recrystallization from boiling ethanol. The measurements were performed on an Oxford Xcalibur Gemini, Eos CCD diffractometer with graphite-monochromated CuKα (λ = 1.54178 Å) radiation. X-ray diffraction intensities were collected (ω scans with ϑ and κ-offsets), integrated and scaled with the CrysAlisPro suite of programs [44]. The unit cell parameters were obtained by least-squares refinement (based on the angular settings for all collected reflections with intensities larger than seven times the standard deviation of measurement errors) using CrysAlisPro. Data were corrected empirically for absorption employing the multi-scan method implemented in CrysAlisPro. The structure was solved by direct methods with SHELXS-97 [45] and the molecular model refined by full-matrix least-squares procedure on F^2 with SHELXL-97 [46]. The hydrogen atoms were located stereo-chemically and refined with the riding model. The methyl H-positions in [$V^{V}O_2$(L3-H)] and ethanol solvent molecules were optimized by treating them as rigid groups which were allowed to rotate during the refinement around the corresponding C–O and C–C bonds. As a result, both CH_3 groups converged to staggered conformations. The position of the ethanol hydroxyl H-atom was refined by rigid rotation of the O–H group around the corresponding O–C bond. The crystal structure data was deposited as CCDC 874914 and contains the supplementary crystallographic data for the structure reported. The data can be obtained free of charge via http://www.ccdc.cam.ac.uk/conts/retrieving.html, or from the Cambridge Crystallographic Data Centre, 12 Union Road, Cambridge CB2 1EZ, UK; fax: (+44) 1223

Please cite this article as: M. Fernández, et al., Oxidovanadium(IV) and dioxidovanadium(V) complexes of tridentate salicylaldehyde semicarbazones: Searching for prospective antitry..., J. Inorg. Biochem. (2013), http://dx.doi.org/10.1016/j.jinorgbio.2013.02.010

336 033; or e-mail: deposit@ccdc.cam.ac.uk. Crystal data and details on data collection and refinement are summarized in Table 1.

2.6. Biological activity

2.6.1. In vitro anti-T. cruzi activity

T. cruzi epimastigotes of the Dm28c strain were maintained in exponential growth at 28 °C in liver infusion tryptose (LIT) medium complemented with 10% (v/v) fetal calf serum (FCS). The effect on cell growth was analyzed incubating an initial concentration of 1×10^6 cells/mL with various concentrations of the compounds for 5 days. Compounds were added as stock DMSO solutions immediately after the preparation of these solutions. The percentage of cell growth was followed by measuring the absorbance, A, of the culture at 595 nm and calculated as follows: $\% = (Ap - A_0p) / (Ac - A_0c) \times 100$, where $Ap = A_{595}$ of the culture containing the drug at day 5; $A_0p = A_{595}$ of the culture containing the drug at day 0; $Ac = A_{595}$ of the culture in the absence of any drug (control) at day 5; $A_0c = A_{595}$ in the absence of the drug at day 0. The results are presented as averages ± SD (standard deviation). The final DMSO concentration in the culture media never exceeded 0.4% (v/v) and had no effect by itself on the proliferation of the parasites [34,35]. Nifurtimox (Nfx) was used as the reference trypanosomicidal drug. Dose–response curves were recorded and the IC_{50} values (50% inhibitory concentration) were determined.

2.6.2. In vitro activity on T. brucei brucei strain 427

The infective form of *T. brucei brucei* strain 427, cell line 449 (encoding one copy of the tet-repressor protein: Pleo^R, [47]), was aerobically cultivated in a humidified incubator at 37 °C with 5% CO_2 in HMI-9 medium supplemented with 10% (v/v) FCS, 10 U/mL penicillin, 10 μg/mL streptomycin and 0.2 μg/mL phleomycin [48]. Ten mM stock solutions of the test compounds were prepared using DMSO as solvent and then diluted in sterile phosphate buffered saline (PBS pH 7.4) to obtain working solutions at 0.5, 0.25 and 0.031 mM. Trypanosomes were grown to late exponential phase and diluted at a cell density of 5×10^5 cells/mL (mid exponential phase) in fresh culture medium. One mL of the cell suspension was plated into each well of a 24-well culture plate. Compounds were immediately added at final concentrations of 25, 5, 3.5, 2.5, 1.25, 0.62 and 0.12 μM. Controls included DMSO at 0.025% (v/v) and culture medium (growth control). Each condition was tested in triplicate. After 24 h incubation at 37 °C with 5% CO_2, living parasites were counted twice with a Neubauer chamber under the light microscope. IC_{50} values were obtained from dose response curves fitted to a sigmoidal equation (Boltzmann model) or extrapolated from linear fitting plots.

Table 1
Crystal data and structure refinement for $[V^VO_2(L3\text{-}H)]\cdot CH_3CH_2OH$.

Empirical formula	$C_{11}\ H_{16}N_3\ O_6\ V$
Formula weight	337.21
Temperature	295(2) K
Wavelength	1.54184 Å
Crystal system	Monoclinic
Space group	$P2_1/c$
Unit cell dimensions	a = 8.4790(8) Å b = 13.538(1) Å c = 12.448(1) Å β = 92.379(7)°
Volume	1427.7(2) Å^3
Z, density (calculated)	4, 1.569 Mg/m^3
Absorption coefficient	6.120 mm^{-1}
F(000)	696
Crystal size	0.15 × 0.12 × 0.07 mm^3
θ-range for data collection	4.83 to 70.97°
Index ranges	$-9 \le h \le 10, -13 \le k \le 16, -15 \le l \le 12$
Reflections collected/unique	5219/2757 [R(int) = 0.0279]
Observed reflections [$I > 2\sigma(I)$]	2067
Completeness to θ = 70.97°	99.8%
Absorption correction	Semi-empirical from equivalents
Max. and min. transmission	1.00000 and 0.74880
Refinement method	Full-matrix least-squares on F^2
Data/ restraints/ parameters	2757/0/191
Goodness-of-fit on F^2	1.066
Final R indices[a] [$I > 2\sigma(I)$]	R1 = 0.0425, wR2 = 0.1131
R indices (all data)	R1 = 0.0583, wR2 = 0.1225
Largest diff. peak and hole	0.402 and −0.380 e.Å^{-3}

[a] $R_1 = \Sigma||F_o| - |F_c||/\Sigma|F_o|$, $wR_2 = [\Sigma w(|F_o|^2 - |F_c|^2)^2/\Sigma w(|F_o|^2)^2]^{1/2}$.

2.7. Lipophilicity studies

Reversed-phase TLC experiments were done on pre-coated TLC plates SIL RP-18W/UV_{254} and eluted with MeOH:DMF:buffer Tris–HCl pH 7.4 (85:5:10, v/v/v). Stock solutions were prepared in pure methanol (Aldrich) prior to use. The plates were developed in a closed chromatographic tank, dried and the spots were located under UV light. The R_f values were averaged from two to three determinations, and converted into R_M via the relationship: $R_M = \log[(1 / R_f) - 1]$ [49–53].

2.8. Atomic force microscopy (AFM) studies

To optimize the observation of the conformational changes in the tertiary structure of pBR322 plasmid DNA, it was heated at 60 °C for 30 min to obtain a majority of open circular form. 15 ng of pBR322 DNA were incubated in an appropriate volume with the required compound concentration corresponding to the molar ratio base pairs (bp): compound 5:1. Each $V^{IV}O$-complex was dissolved in a minimal amount of DMSO, and (4-(2-hydroxyethyl)-1-piperazineethanesulfonic acid buffer (HEPES) pH 7.4 was then added up to the required concentration. The different solutions as well as Milli-Q® water were filtered with 0.2 μm FP030/3 filters (Schleicher & Schuell GmbH, Germany). Incubations were carried out at 37 °C for 24 h.

Samples were prepared by placing a drop of DNA solution or DNA-compound solution onto mica (TED PELLA, INC. California, USA). After adsorption for 5 min at room temperature, the samples were rinsed for 10 s in a jet of deionised water (18 MΩ cm^{-1} from a Milli-Q® water purification system) directed onto the surface. The samples were blow dried with compressed argon and then imaged by AFM.

The samples were imaged by a Nanoscope III Multimode AFM (Digital Instrumentals Inc., Santa Barbara, CA) operating in tapping mode in air at a scan rate of 1–3 Hz. The AFM probe was 125 mm-long monocrystalline silicon cantilever with integrated conical shaped Si tips (Nanosensors GmbH Germany) with an average resonance frequency $f_o = 330$ kHz and spring constant $K = 50$ N/m. The cantilever was rectangular and the tip radius given by the supplier was 10 nm, a cone angle of 35° and high aspect ratio. The images were obtained at room temperature ($T = 23 \pm 2$ °C) and the relative humidity was usually lower than 40% [33,35].

3. Results and discussion

Nine vanadium complexes of the tridentate salicylaldehyde semicarbazone derivatives L3–L5 (Fig. 1a) were synthesized with reasonable yields. All of them are non conducting compounds in DMF. Analytical, TGA (thermogravimetric analysis) and FTIR and ^{1}H NMR spectroscopic results of the three V^VO_2-complexes are in agreement with the proposed formula, $[V^VO_2(L\text{-}H)]\cdot xH_2O$, and their molecular formulae are presented in Fig. 1b. Moreover, analytical, TGA and ESI-MS, FTIR and EPR spectroscopic results of the six new $V^{IV}O$-complexes are in agreement with the proposed formulation: $[V^{IV}O(L\text{-}2H)(NN)]\cdot xH_2O$, and their molecular formulae are also depicted in Fig. 1c. ESI-MS experiments allowed the clear detection of the molecular ion for each $V^{IV}O$-complex. In the case of complexes **6** and **9**, containing the brominated ligand L5, two peaks were detected for M + H, reflecting the isotope distribution of ^{79}Br and ^{81}Br.

3.1. Characterization of the complexes in the solid state

3.1.1. Thermal analysis

Thermogravimetric curves for $[V^{V}O_2(L\text{-}H)]$, where L = L3 or L4, demonstrated the absense of crystallization solvent molecules. $[V^{V}O_2(L5\text{-}H)]$ showed a single weight loss of 5.8% (calcd. 5.6%), centered near 50 °C, that corresponds to one water molecule. On the other hand, the complexes of the $[V^{IV}O(L\text{-}2H)(bipy)]$ series showed also a single weight loss that corresponds to the number of water molecules assigned in each case (see above).

3.1.2. IR spectroscopic studies

Based on our previous reports on vibrational behavior of metal complexes of salicylaldehyde semicarbazone derivatives [34–39,54] and other reports [55,56], tentative assignments were made. Some selected IR bands and their tentative assignments are presented in Table 2. The absence of the ν(C═O) bands, present in the ligands at around 1667–1676 cm^{-1}, indicates the enolization of the amide functionality upon coordination to vanadium. Instead strong bands at *ca.* 1600–1664 cm^{-1} are observed which are characteristic of the coordination of the ligand enolate forms [55].

In the case of the $[V^{V}O_2(L\text{-}H)]$ complexes, the shift of ν(C═O) and ν(C═N) bands and the non-observation of the ν(OH) (in the 3430–3500 cm^{-1} region) are in agreement with tridentate coordination through the carbonylic oxygen ($O_{C=O}$), the azomethyne nitrogen ($N_{azomethyne}$) and the phenolic oxygen ($O_{phenolate}$), and with deprotonation of the semicarbazone ligand at the phenolic hydroxyl group. The $[V^{IV}O(L\text{-}2H)(NN)]$ complexes show a similar spectroscopic behavior but in addition deprotonation of the NH group is confirmed by the non-observation of the NH stretching band in the 3160–3180 cm^{-1} region upon complexation. In these V^{IV}-complexes the semicarbazones act as double deprotonated tridentate ligands. In addition, $[V^{V}O_2(L\text{-}H)]$ complexes show two bands assigned to the symmetric and antisymmetric stretching that are characteristic of the VO_2^+ moiety. $[V^{IV}O(L\text{-}2H)(NN)]$ complexes show a characteristic intense band around 960 cm^{-1} assigned to ν(V═O). All the spectral modifications observed upon complexation agree with those previously reported for the L1 and L2 analogous $[V^{V}O_2(L\text{-}H)]$ and $[V^{IV}O(L\text{-}2H)(NN)]$ complexes [34–37].

3.1.3. Crystal structure of $[V^{V}O_2(L3\text{-}H)]\cdot CH_3CH_2OH$

Bond distances and angles around vanadium(V) ion in $[V^{V}O_2(L3\text{-}H)]\cdot CH_3CH_2OH$ are shown in Table 3. Fig. 2 is an ORTEP [57] drawing of the complex.

The dioxidovanadium(V) cation, VO_2^+, shows the expected angular conformation with V–O bond lengths of 1.509(2) and 1.649(2) Å and a O–V–O angle of 108.4(1)°. The V^{V} center is coordinated to a 3-methoxysalicylaldehyde semicarbazone (**L**) anion acting as tridentate ligand through its phenol and carbonyl oxygen atoms [V–$O_{phenolato}$ and V–$O_{C=O}$ distances of 1.888(2) and 2.000(2) Å] and the azomethyne nitrogen atom [V–N1 distance of 2.173(2) Å]. The ligand is nearly planar [*rms* deviation of atoms from the best least-squares plane equal to 0.084 Å]. The metal ion departs slightly from the plane of (O2, O3, N1, O4) by 0.231(2) Å toward the strongest bound-to-metal VO_2^+ oxygen (O1), which is 1.798(3) Å apart from the plane.

The crystal structure of the compound is further stabilized by a network of O–H···O, N2–H···O, and N3–H···O bonds. Detailed H-bond distances and angles are provided as supplementary information (Table S7).

3.2. Characterization of the complexes in solution

As the biological activity of the complexes was tested in vitro in aerated diluted solutions and with incubating periods of several days, efforts were done to characterize the complexes in solution and, particularly, to understand the stability of the $[V^{IV}O(L\text{-}2H)(NN)]$ complexes towards hydrolysis and/or oxidation of V^{IV}. In fact the biologically active species may differ significantly from the solid complex that undergoes dissolution.

The $V^{V}O_2$-complexes were characterized in solution by ^1H NMR and HETCOR experiments. Their stability in solution was followed by the same technique. To characterize the ligand substitution ability of the $[V^{IV}O(L\text{-}2H)(NN)]$ complexes in solution, EPR and ^{51}V NMR studies were also carried out with fresh and aged DMF (and in some cases DMSO) solutions of the complexes. In addition, the results were compared with those obtained from the stability studies done with both series of mixed-ligand compounds by measuring the conductivity of DMSO-H_2O and DMSO solutions during 5 days.

3.2.1. NMR characterization of the $[V^{V}O_2(L\text{-}H)]$ complexes, **1**–*3*

NMR spectroscopic data show narrow signals, typical of diamagnetic complexes. HETCOR experiments allowed the assignment of all ^1H signals for the studied complexes. The ^1H NMR chemical shift values along with the chemical shift differences between each complex and the corresponding ligand (expressed as $\Delta\delta$) are listed in Table 4. The figure depicted in the table shows the numbering scheme of the salicylaldehyde semicarbazone moiety. ^1H NMR integrations and signal multiplicities are in agreement with the proposed molecular formula. The three complexes show similar ^1H chemical shifts of the salicylaldehyde semicarbazone common fragment of their molecules. As previously discussed for $V^{V}O_2$-complexes of L1 and L2 derivatives, upon coordination, the de-shielding effect of the metal is apparent in some protons (i.e. protons 1, 8, 10 and 11), causing a down-field shift of the corresponding ^1H NMR peaks [36,37]. The up-field shift of proton 3 may be the result of a decreasing azomethyne anisotropic effect in the coordinated form of L. When L is coordinated, the azomethyne moiety is fixed in an opposite spatial distribution to proton 3. Therefore, upon coordination this proton is less affected by the magnetic anisotropy of the C═N double bond than in the free ligand.

Table 2
Tentative assignment of selected IR bands of the $[V^{V}O_2(L\text{-}H)]$ and $[V^{IV}O(L\text{-}2H)(NN)]$ complexes, **1**–**9**. Bands for the free semicarbazone ligands L3–L5 are included for comparison. Band positions are given in cm^{-1}.

Compound	$\nu(VO_2)_s$	$\nu(VO_2)_{as}$	ν(VO)	ν(C═O)	ν(C═N)[a]	ν(O–H)	ν(N–H)
L3	–	–	–	1676	1586	3466	3171
$[V^{V}O_2(L3\text{-}H)]$, **1**	895	942	–	1662	1555	–	3200
$[V^{IV}O(L3\text{-}2H)(bipy)]$, **4**	–	–	958	1607	1550	–	–
$[V^{IV}O(L3\text{-}2H)(dppz)]$, **7**	–	–	959	1610	1551	–	–
L4	–	–	–	1667	1595	3433	3160
$[V^{V}O_2(L4\text{-}H)]$, **2**	876	892	–	1654	1558	–	3174
$[V^{IV}O(L4\text{-}2H)(bipy)]$, **5**	–	–	960	1600	1550	–	–
$[V^{IV}O(L4\text{-}2H)(dppz)]$, **8**	–	–	965	1610	1543	–	–
L5	–	–	–	1672	1572	3477	3190
$[V^{V}O_2(L5\text{-}H)]$, **3**	849	889	–	1664	1550	–	3200
$[V^{IV}O(L5\text{-}2H)(bipy)]$, **6**	–	–	959	1630	1541	–	–
$[V^{IV}O(L5\text{-}2H)(dppz)]$, **9**	–	–	961	1614	1538	–	–

[a] The bands assigned to ν(C═N) (azomethine) are associated with the aromatic (C═C) stretching bands [56]. Crystallization solvent molecules were not included for simplicity.

Please cite this article as: M. Fernández, et al., Oxidovanadium(IV) and dioxidovanadium(V) complexes of tridentate salicylaldehyde semicarbazones: Searching for prospective antitry..., J. Inorg. Biochem. (2013), http://dx.doi.org/10.1016/j.jinorgbio.2013.02.010

ARTICLE IN PRESS

Table 3
Bond lengths [Å] and angles around vanadium(V) [°] in $[V^{V}O_2(L3\text{-}H)]\cdot CH_3CH_2OH$.

Bond distances	
V–O(1)	1.590(2)
V–O(2)	1.649(2)
V–O(3)	1.888(2)
V–O(4)	2.000(2)
V–N(1)	2.173(2)
Bond angles	
O(1)–V–O(2)	108.4(1)
O(1)–V–O(3)	104.6(1)
O(2)–V–O(3)	99.7(1)
O(1)–V–O(4)	98.0(1)
O(2)–V–O(4)	90.7(1)
O(3)–V–O(4)	150.5(1)
O(1)–V–N(1)	106.2(1)
O(2)–V–N(1)	143.5(1)
O(3)–V–N(1)	82.42(9)
O(4)–V–N(1)	73.15(9)

This effect has been also previously observed for $V^{V}O_2$-complexes of the related salicylaldehyde semicarbazones L1 and L2 [36,37]. As expected, proton 7 is not observed in the spectra of the three complexes.

The $V^{V}O_2$-compounds showed similar NMR spectra after 5 days of preparation of the solutions, which indicates their high stability in solution.

3.2.2. EPR characterization of the $[V^{IV}O(L\text{-}2H)(NN)]$ complexes, 4–9

EPR spectroscopy of $V^{IV}O$-complexes is a powerful tool to get structural information on the binding mode of the species present in solution [58]. The additivity relationship, first proposed by Wüthrich [59] and later refined by Chasteen [42], correlates the hyperfine coupling constant, namely A_z with the electron-donating ability of the ligands present in the equatorial plane of the $V^{IV}O$-center. The A_z value can be estimated as $A_z^{est} = \sum A_{z,i}$ (i = 1 to 4), $A_{z,i}$ being the specific contribution of each donor atom equatorially bound to V^{IV}. Care must be taken when applying this relationship as it may be difficult to distinguish between different donor groups with similar $A_{z,i}$ values [42,58,60–62]. The estimated error in the $A_{z,i}$ values is $\pm 3 \times 10^{-4}$ cm^{-1}.

The spectra of the $V^{IV}O$-mixed-ligand complexes exhibit a hyperfine pattern typical of $V^{IV}O$-complexes, consistent with the presence of monomeric $V^{IV}O$-bound species with d^1_{xy} ground-state configuration.

Fig. 3 shows the EPR spectra (at 77 K) obtained for 3 mM solutions of the bipy-containing complexes in DMF. The spectra of these complexes show the presence of two species, particularly evident in the case of **4** and **5**. The spin Hamiltonian parameters of the spectra are included in Table 5. The *g* and *A* parameters obtained for the dppz-containing complexes and the inner (major) species of the bipy-containing complexes are the same within experimental error indicating the same binding set for all of them. They are also very close to those previously reported for the related phenanthroline compounds [35] and for the bipy-containing complexes of L1 and L2, for which two species were also detected. Thus we propose the same binding set: the semicarbazone acting as a tridentate ligand, binding through $O_{phenolate}$, $N_{azomethyne}$ and $O_{enolato}$ in the equatorial plane and the NN co-ligands binding with one N in the equatorial position and the other *trans* to the O_{oxido} donor. The A_z^{est} for this binding set is 158.5×10^{-4} cm^{-1} {considering $O_{phenolate} = 38.9 \times 10^{-4}$ cm^{-1}, $N_{NN} = 40.4 \times 10^{-4}$ cm^{-1}, $N_{azomethyne} = 41.6 \times 10^{-4}$ cm^{-1}, $O_{enolate} = 37.6 \times 10^{-4}$ cm^{-1}} [2,42,58,60,62,63] and fits the experimental values, within the estimated error.

The minor species, present in the spectra of the bipy-containing complexes shows higher A_z values (ca. 166.7×10^{-4} cm^{-1}), and its spin Hamiltonian parameters are similar to those also obtained for the minor species of $V^{IV}O(L\text{-}2H)(bipy)$ (with L = L1 and L2), [34] suggesting significant solvolysis and substitution of the bipy ligand by DMF. Nevertheless, the main complex species detected in freshly prepared solutions correspond to the formulation $[V^{IV}O(L\text{-}2H)(bipy)]$. The V^{IV}-dppz-containing complexes show only the presence of one species, $[V^{IV}O(L\text{-}2H)(dppz)]$, and no solvolysis was detected for the EPR active species.

3.3. Accessing the stability of the complexes in solution

3.3.1. Conductivity measurements of the $[V^{IV}O(L\text{-}2H)(NN)]$ complexes, 4–9

Conductivity measurements carried out with 10^{-4} M solutions in DMSO and 8% DMSO-H_2O show that changes due to substitution of ligands due to solvolysis or oxidation processes occur significantly more slowly in 8% DMSO-H_2O than in neat DMSO solution. After 5 days the conductivity of the $[V^{IV}O(L\text{-}2H)(NN)]$ solutions showed only a very slight increase in respect to t = 0 value, probably due to generation of hydrolyzed V^{V} charged species. On the other hand, the solutions in neat DMSO showed a continuous increase of their conductivity which was clearly detectable after 24 h of preparation of the solution.

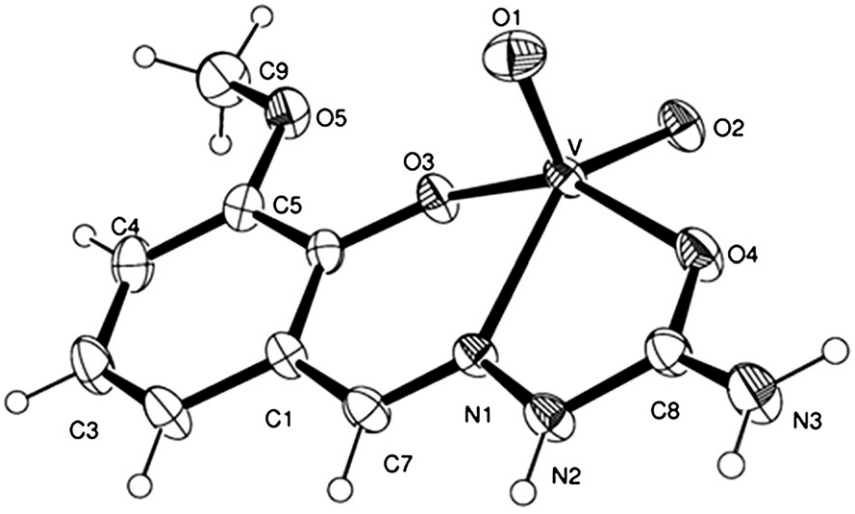

Fig. 2. ORTEP drawing depicting a view of $[V^{V}O_2(L3\text{-}H)]$ showing the labeling of the non-H atoms and their displacement ellipsoids at the 50% probability level.

Please cite this article as: M. Fernández, et al., Oxidovanadium(IV) and dioxidovanadium(V) complexes of tridentate salicylaldehyde semicarbazones: Searching for prospective antitry..., J. Inorg. Biochem. (2013), http://dx.doi.org/10.1016/j.jinorgbio.2013.02.010

Table 4
^{1}H NMR chemical shifts (δ, ppm) of $[V^VO_2(L\text{-}H)]$ complexes in DMSO-d_6 at 30 °C.

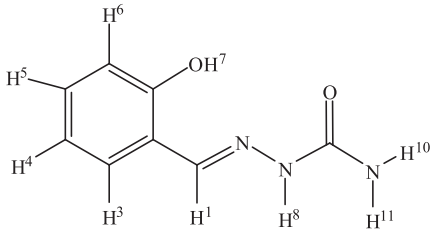

	$[V^VO_2(L3\text{-}H)]$			$[V^VO_2(L4\text{-}H)]$			$[V^VO_2(L5\text{-}H)]$		
H	δ_{ligand}	$\delta_{complex}$	$\Delta\delta^a$	δ_{ligand}	$\delta_{complex}$	$\Delta\delta^a$	δ_{ligand}	$\delta_{complex}$	$\Delta\delta^a$
1	8.17	8.59	0.42	8.17	8.59	0.42	8.11	8.51	0.40
3	7.38	7.09	−0.29	7.34	7.05	−0.29	7.69	7.34	−0.35
4	6.77	6.79	0.02	6.75	6.77	0.02	–	–	–
5	6.92	7.06	0.14	6.92	7.04	0.12	7.06	7.12	0.06
7	9.30	–	–	9.19	–	–	9.47	–	–
8	10.22	12.48	2.26	10.21	12.48	2.27	10.28	12.61	2.33
10	6.41	7.97	1.56	6.41	7.09	0.68	6.53	8.24	1.71
11									
CH_3	3.80	3.75	−0.05	1.35	1.34	−0.01	3.83	3.77	−0.06
CH_2	–	–	–	4.06	4.03	−0.03		–	–

[a] $\Delta\delta = \delta_{complex} - \delta_{ligand}$.

3.3.2. Stability of the $V^{IV}O$-complexes towards solvolysis and/or oxidation

To evaluate the stability of the $V^{IV}O$-complexes towards oxidation, the EPR and visible absorption spectra were measured during one day period.

Strong charge transfer bands appear up to ca. 650 nm in the visible absorption spectra of the solutions of $[V^{IV}O(L\text{-}2H)(NN)]$ in DMF, therefore distinct detectable maxima corresponding to d–d transitions cannot be identified. The visible absorption spectra change with time but faster for the solutions of the bipy-containing complexes than for the corresponding dppz-containing compounds; e.g. with a 3 mM solution of $[V^{IV}O(L4\text{-}2H)(bipy)]$ the absorption at 780 nm decreased ca. 52% after 3 h, while with $[V^{IV}O(L4\text{-}2H)(dppz)]$ this decrease was ca. 30%.

Fig. 4 shows the changes in the EPR spectra observed for complex **7**. After 3 h the intensity of the spectrum decreases, but ca. 25% of the complex is still in the +4 oxidation state and the spin Hamiltonian parameters are the same. After 6 h the oxidation is almost complete. For the other complexes the behavior was similar.

Having detected solvolysis and oxidation of the complexes in solution by EPR, ^{51}V NMR spectroscopy was used to detect probable oxidation products after aging aerated DMF solutions. All bipy-containing samples show quite intense peaks at ca. − 533 ppm after 24 h (Table 5). The dppz samples, besides this resonance, show the presence of other peaks, which can be tentatively assigned to vanadate oligomers [at ca. −557 ppm (V_1) and −570 ppm (V_4)]. The main peak is in the expected range for monomeric V^VO_2-complexes involving N,O-ligands [2]. Moreover, chemical shifts of V^VO_2-semicarbazone complexes have been reported and theoretically predicted in the −530 to −550 ppm range [64]. Thus the V^V-complexes formed with δ_V values in the range of −529 to −534 ppm probably correspond to species formulated as $V^VO_2(L\text{-}2H)(solvent)$.

From the experiments made we can conclude that the $[V^{IV}O(L\text{-}2H)(bipy)]$ complexes, where L = L3–L5, are significantly more susceptible to oxidation and solvolysis in DMF solution than the corresponding $[V^{IV}O(L\text{-}2H)(dppz)]$ and $[V^{IV}O(L\text{-}2H)(phen)]$ complexes [35], and similar to the structurally related $[V^{IV}O(L\text{-}2H)(bipy)]$ complexes of L1 and L2 [34]. The $[V^{IV}O(L\text{-}2H)(dppz)]$ complexes are less stable towards oxidation than the corresponding phenanthroline complexes, since e.g. complex $[V^{IV}O(L2\text{-}2H)(phen)]$, shows no considerable oxidation even after 72 h in DMF [35], and the V^{IV}-dppz complexes oxidize within 6 h.

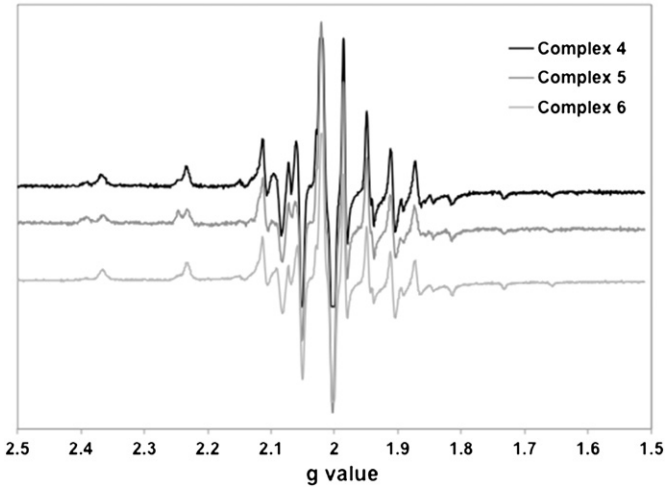

Fig. 3. 1st derivative EPR spectra of frozen solutions (77 K) of $[V^{IV}O(L\text{-}2H)(bipy)]$ complexes, **4**–**6**, after dissolution in DMF (ca. 3 mM).

3.4. Lipophilicity studies

Among the prime factors controlling transport to and interaction with biological receptors are lipophilic, polar, electronic and steric ones. Hence, many quantitative structure activity relationships contain terms representing more than one of these factors [65]. Herein, due to the chemodiversity of the used ligands and, thus, their effect on physicochemical properties such as lipophilicity, this property was determined for the whole series of chemically related $V^{IV}O$ mixed-ligand complexes developed up to now to analyze its effect on the biological activity. Lipophilicity was experimentally determined using reversed-phase TLC experiments where the stationary phase, pre-coated TLC-C_{18}, simulates lipids of biological membranes or receptors, and the mobile phase, MeOH:DMF:buffer Tris–HCl pH 7.4 (85:5:10, v/v/v), resembles the aqueous biological milieu. Several attempts were done to select the adequate mobile phase, which allowed it to differentiate complexes according to their lipophilicity, the more adequate one being a combination of polar organic solvents, MeOH and DMF, with a buffer that simulates the physiological pH

Please cite this article as: M. Fernández, et al., Oxidovanadium(IV) and dioxidovanadium(V) complexes of tridentate salicylaldehyde semicarbazones: Searching for prospective antitry..., J. Inorg. Biochem. (2013), http://dx.doi.org/10.1016/j.jinorgbio.2013.02.010

Table 5
^{51}V NMR chemical shifts, δ_V, 24 h after dissolution in DMSO, and EPR spin Hamiltonian parameters.

Complex	δ_V/ppm[a]	g_x, g_y	g_z	A_x, $A_y \times 10^4/cm^{-1}$	$A_z \times 10^4/cm^{-1}$
$[V^{IV}O(L3\text{-}2H)(bipy)]$, **4**	−533	1.982	1.951	55.2	160.2 166.7[b]
$[V^{IV}O(L4\text{-}2H)(bipy)]$, **5**	−534	1.982	1.951	54.8	159.4
$[V^{IV}O(L5\text{-}2H)(bipy)]$, **6**	−533	1.979	1.947	56.3	161.2
$[V^{IV}O(L3\text{-}2H)(dppz)]$, **7**[c]	−529, −558[d], −571[d]	1.976	1.947	54.8	159.2
$[V^{IV}O(L4\text{-}2H)(dppz)]$, **8**[c]	−528, −556[d], −568[d]	1.976	1.947	55.8	159.7
$[V^{IV}O(L5\text{-}2H)(dppz)]$, **9**[c]	−529, −558[d]	1.976	1.948	54.7	159.6

[a] See Section 3.3.2.
[b] A_z for the minor (outer) species.
[c] The spin Hamiltonian parameters were obtained by an iterative procedure (see text).
[d] Minor peaks.

value. The R_f values obtained were converted into R_M values via the relationship: $R_M = \log [(1 / R_f) - 1]$. Table 6 summarizes R_M for each compound.

When the complete series of evaluated compounds, i.e. complexes, ligands and Nifurtimox (Table 6), were analyzed to find a correlation between R_M and the anti-*T. cruzi* activity no statistically significant equations were obtained. However, when the population under study was restricted to the $V^{IV}O$-complexes a clear quadratic correlation was found ($IC_{50} = 2495 \pm 781–3477 \pm 1161\ R_M + 1208 \pm 425\ R_M^2$, $r^2_{adj} = 0.6381$, $F = 13.34$, $p = 0.0009$, Fig. 5). Similar nearly parabolic relationship between biological response and lipophilicity has been previously described for a large number of biologically relevant families of compounds [49,53,66]. From this correlation an optimum R_M value, close to 1.44 (Fig. 5), was obtained as a design tool for further development of new compounds that could possess a better biological profile.

3.5. Biological results

3.5.1. In vitro anti-T. cruzi activity

The complexes were evaluated in vitro for their anti-*T. cruzi* activities against epimastigotes of Dm28c strain. The results were compared to that of the reference drug Nifurtimox and to those previously reported for related $[V^{IV}O(L\text{-}2H)(NN)]$ complexes (Table 6). The free semicarbazones L1–L5 were previously tested by the same in vitro test and showed no significant inhibitory effect on *T. cruzi* epimastigotes ($IC_{50} > 100$ μM) [33,35] and the bipy and dppz ligands showed IC_{50} values of ca. 70 μM and 3 μM, respectively [33,34]. The precursor $[VO(acac)_2]$ as well as all the $[VO_2(L\text{-}H)]$ complexes tested in this work, including the new compounds **1–3**, were not toxic against *T. cruzi* ($IC_{50} > 100$ μM). The newly synthesized $[V^{IV}O(L\text{-}2H)(bipy)]$ complexes (L = L3–L5) showed low anti-*T.cruzi* activity with similar IC_{50} values to the previously reported L1 and L2 analogous bipy-containing complexes and higher IC_{50} values than Nifurtimox

Table 6
In vitro biological activity on *T. cruzi* (Dm28c strain) and lipophilicity of the oxidovanadium(IV) complexes. Nifurtimox was included for comparison.

Compound	$IC_{50} \pm SD$ (μM)	R_M
$[V^{IV}O(L1\text{-}2H)(bipy)]$	73 [34]	1.205
$[V^{IV}O(L2\text{-}2H)(bipy)]$	84 [34]	1.149
$[V^{IV}O(L3\text{-}2H)(bipy)]$	76.2 ± 9.7	1.134
$[V^{IV}O(L4\text{-}2H)(bipy)]$	161 ± 57	1.161
$[V^{IV}O(L5\text{-}2H)(bipy)]$	58.0 ± 14.8	1.193
$[V^{IV}O(L1\text{-}2H)(dppz)]$	13 [34]	1.590
$[V^{IV}O(L2\text{-}2H)(dppz)]$	19 [34]	1.560
$[V^{IV}O(L3\text{-}2H)(dppz)]$	4.70 ± 3.35	1.405
$[V^{IV}O(L4\text{-}2H)(dppz)]$	12.7 ± 8.27	1.560
$[V^{IV}O(L5\text{-}2H)(dppz)]$	5.05 ± 1.60	1.537
$[V^{IV}O(L1\text{-}2H)(phen)]$	2.0 [35]	1.221
$[V^{IV}O(L2\text{-}2H)(phen)]$	3.1 [35]	1.559
$[V^{IV}O(L3\text{-}2H)(phen)]$	2.3 [35]	1.509
$[V^{IV}O(L4\text{-}2H)(phen)]$	1.6 [35]	1.352
$[V^{IV}O(L5\text{-}2H)(phen)]$	3.8 [35]	1.340
Nifurtimox	6.0 [35]	1.221

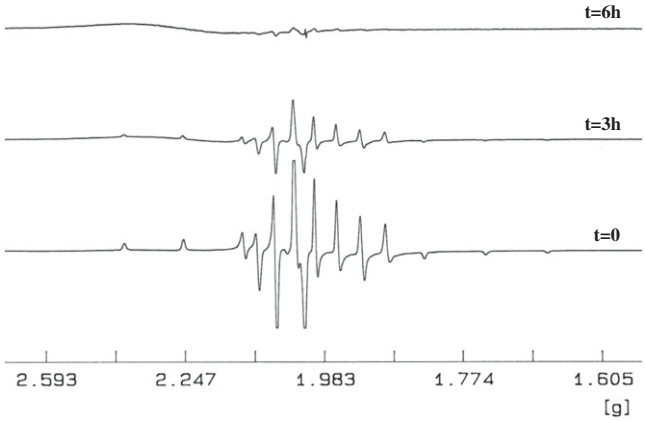

Fig. 4. Changes observed with time in the EPR spectra of a frozen solution (100 K) of complex $[V^{IV}O(L3\text{-}2H)(dppz)]$, **7**, after dissolution in DMF (ca. 3 mM).

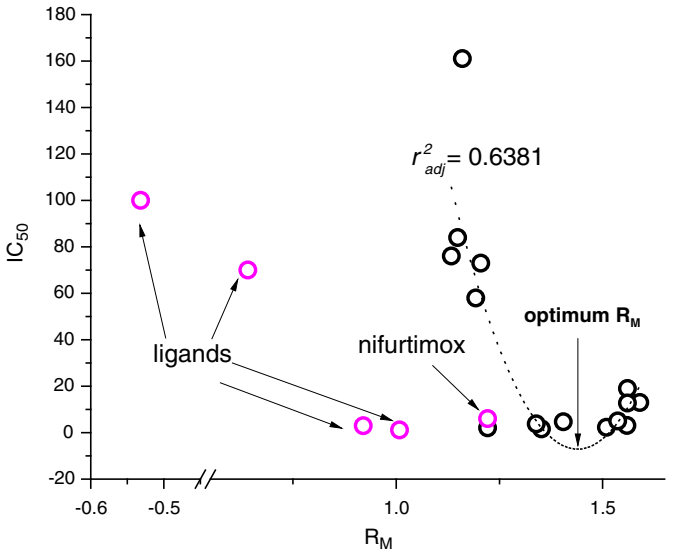

Fig. 5. IC_{50} values (in μM units) for the anti-*T. cruzi* activity of the compounds vs R_M values as a measure of their lipophilicity.

Table 7
In vitro activity on *T. brucei brucei* (strain 427) of the $V^{IV}O$-complexes.

Compound	$IC_{50} \pm SD$ (μM)
$[V^{IV}O(L3\text{-}2H)(bipy)]$	>25
$[V^{IV}O(L4\text{-}2H)(bipy)]$	>25
$[V^{IV}O(L5\text{-}2H)(bipy)]$	>25
$[V^{IV}O(L3\text{-}2H)(dppz)]$	2.8 ± 0.1
$[V^{IV}O(L4\text{-}2H)(dppz)]$	3.0 ± 0.2
$[V^{IV}O(L5\text{-}2H)(dppz)]$	1.5 ± 0.1

[34]. On the other hand, the $[V^{IV}O(L\text{-}2H)(dppz)]$ complexes showed IC_{50} values lower or of the same order than Nifurtimox and similar to those previously reported for the L1 and L2 analogous dppz compounds [34]. The substitution on the phenol moiety of the semicarbazone ligand seems to have only a low incidence on the antitrypanosomal activity. In addition, the activity of the bipy mixed-ligand complexes is significantly lower than that of the analogous compounds with other NN ligands, like dppz and phen, indicating that the nature of this co-ligand is determinant of the biological activity (Table 6) [33,35].

The biological activity of the compounds thus appears to correlate with the stability of the $[V^{IV}O(L\text{-}2H)(NN)]$ complexes. Globally the phen-containing compounds are the most stable and the most active. These are followed in stability and activity by the dppz-containing ones, and finally the bipy-containing complexes, which are the least stable and with lower activity. Whether this is due to an intrinsic bioactivity of the $[V^{IV}O(L\text{-}2H)(NN)]$ species or to a higher bioavailability is not presently known, however, as shown, the lipophilicity of the compounds appears to be correlated with the biological activity. Inside cells the vanadium speciation (not addressed in this work) may yield species containing or not the original ligands. The NN moieties may be relevant in this respect, and there are several examples where phen and other related compounds, which may act as DNA intercalators, improve the biological activity of the metal-based systems.

3.5.2. In vitro anti-T. brucei activity

The new dppz-containing $V^{IV}O$-complexes showed growth inhibitory activity towards *T. brucei brucei*. In fact they induced a dose-dependent antiproliferative effect on parasites treated for 24 h

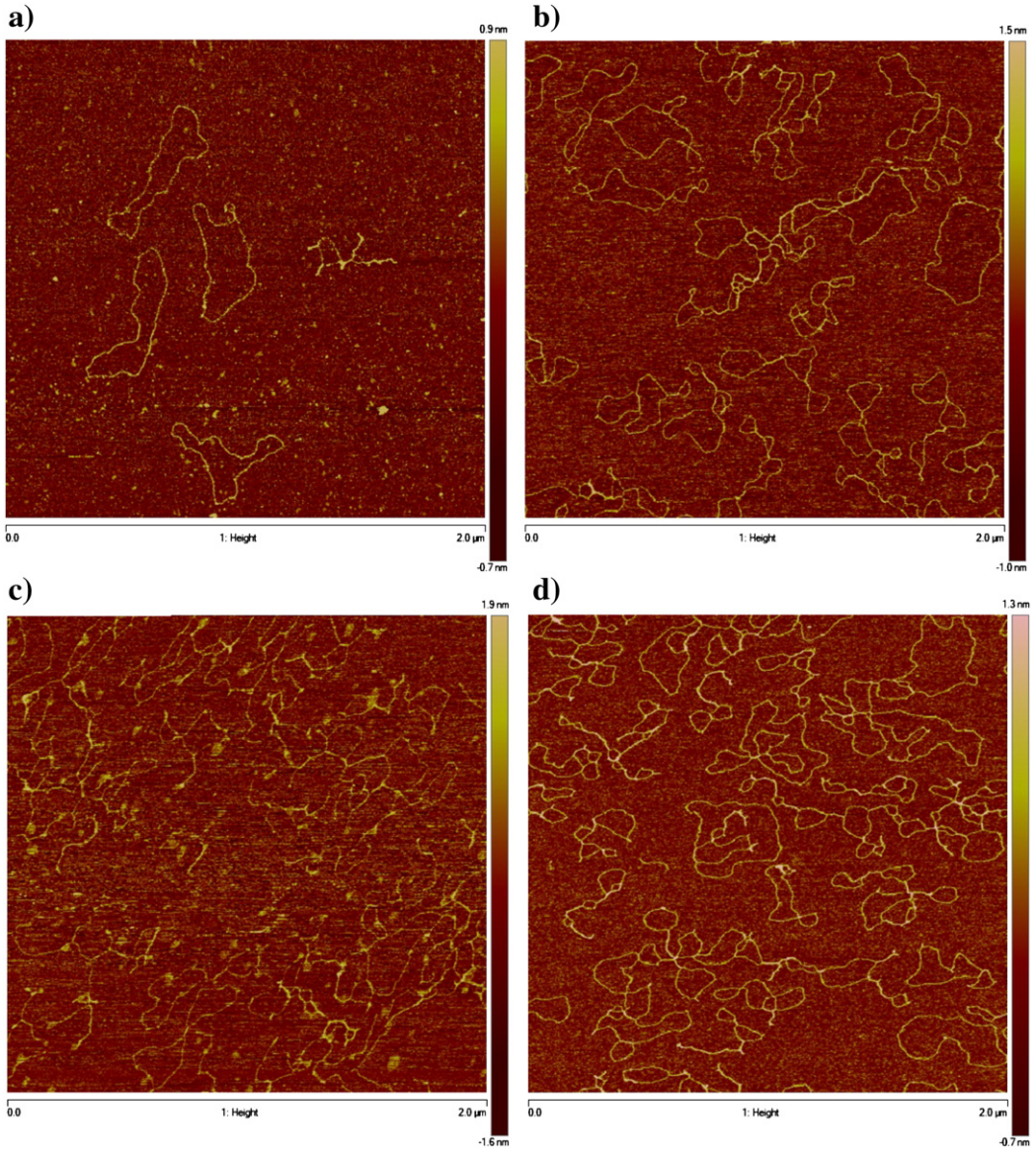

Fig. 6. AFM images showing the modifications suffered by pBR322 DNA due to the interaction with the dppz-containing $V^{IV}O$-compounds: a) pBR322 DNA b) **7**, $[V^{IV}O(L3\text{-}2H)(dppz)]$, c) **8**, $[V^{IV}O(L4\text{-}2H)(dppz)]$, d) **9**, $[V^{IV}O(L5\text{-}2H)(dppz)]$ for molar ratio compound: DNA base pairs 1:5 and 24 h incubation at 37 °C.

Please cite this article as: M. Fernández, et al., Oxidovanadium(IV) and dioxidovanadium(V) complexes of tridentate salicylaldehyde semicarbazones: Searching for prospective antitry..., J. Inorg. Biochem. (2013), http://dx.doi.org/10.1016/j.jinorgbio.2013.02.010

ARTICLE IN PRESS

(Table 7). They show IC_{50} values in the low micromolar range. On the contrary, the analogous bipy-containing complexes showed no significant activity against bloodstream *T. brucei*.

The behavior of these bipy- and dppz-containing complexes against *T. brucei* is similar to the one observed against *T. cruzi*. These results support our drug design approach that involves the development of compounds that could show activity towards both genetically related parasites.

3.6. Atomic force microscopy (AFM) results

AFM has proved to be a useful tool for imaging DNA and also DNA interactions with metal complexes [67,68]. As mentioned above, the present series of $[V^{IV}O(L\text{-}2H)(NN)]$ complexes was developed aiming to target DNA. To confirm that DNA is a potential parasite target, the interaction of the new bioactive complexes $[V^{IV}O(L\text{-}2H)(dppz)]$ with DNA was preliminarily studied by AFM using pBR322 plasmid as model molecule. AFM images are depicted in Fig. 6. The three complexes modified the tertiary structure of the plasmid. This is visualized as changes in the DNA shape, such as crosslinking and supercoiling. The observed effect is only slightly affected by the nature of the semicarbazone co-ligand. These observations thus indicate that the $[V^{IV}O(L\text{-}2H)(dppz)]$ compounds interact with DNA but more studies involving other techniques are needed in order to clearly establish DNA as a target.

4. Conclusions

A series of $[V^{V}O_2(L\text{-}2H)]$ and of mixed-ligand $V^{IV}O$-complexes, $[V^{IV}O(L\text{-}2H)(NN)]$, including tridentate salicylaldehyde semicarbazone derivatives as ligands (L) and either bipy or dppz as co-ligands (NN), were prepared and characterized. The new $[V^{IV}O(L\text{-}2H)(dppz)]$ complexes showed IC_{50} values in the low micromolar range against *T. cruzi* epimastigotes being about ten to fifteen times more toxic to the parasite than the bipy-containing analogues. The former also showed quite good in vitro activity on *T. brucei brucei* (strain 427). The corresponding $V^{V}O_2$-complexes, $[V^{V}O_2(L\text{-}2H)]$ do not show activity towards *T. cruzi* epimastigotes (Dm28c strain).

Globally the data suggest that the relevant species for biological activity are the $[V^{IV}O(L\text{-}2H)(NN)]$ compounds including the bidentate NN co-ligand, the order of activity of the complexes being phen-containing > dppz-containing > bipy-containing compounds. This order correlates with the order of stability of the $V^{IV}O$-complexes against solvolysis and oxidation, as accessed by the visible absorption, EPR and ^{51}V NMR studies carried out.

The complexes were shown to interact with DNA, suggesting that this biomolecule may be the parasite target.

Taking into account several other $[V^{IV}O(L\text{-}2H)(NN)]$ complexes previously studied by us, the lipophilicity of the compounds correlated with the biological activity observed. The nature of the NN ligand is particularly relevant, but not much the substitution on the salicylaldehyde semicarbazone moiety [34,35]. A parabolic relationship between biological response and lipophilicity was obtained and, from this correlation an optimum R_M value, close to 1.44, was determined, which may be used as design guide for future development of new compounds toward a better biological profile.

Acknowledgments

Authors would like to thank RIIDFCM CYTED (209RT0380) network for supporting collaborative research on development of bioactive metal-based compounds and RIDIMEDCHAG CYTED, and also the financial support of Fundação para a Ciência e Tecnologia (FCT, Portugal), PEst-OE/QUI/UI0100/2011 and CIÊNCIA2007, and the Portuguese NMR and Mass Spectrometry Networks (IST-UTL Centers). The crystallographic work was supported by CONICET (PIP 1529), and by ANPCyT (PME06 2804 and PICT06 2315) of Argentina. G.A.E. and O.E.P are research fellows of CONICET. M.A.C. acknowledges the support of the Agencia Nacional de Investigación e Innovación (ANII; Innova Uruguay, Agreement No. DCI-ALA/2007/19.040 between Uruguay and the European Commission). AFM studies were supported by Ministerio de Economía y Competitividad (MINECO, CTQ2011-27929-C02-01) and performed by Rosa Brissos. M.F. acknowledges the support of the Agencia Nacional de Investigación e Innovación (ANII, Uruguay) grant ilNI_X_2010_2_3105.

Appendix A. Supplementary data

Tables containing crystallographic information for $[V^{V}O_2(L3\text{-}H)]\cdot CH_3CH_2OH$, including atomic coordinates and equivalent isotropic displacement parameters (Table S3), intra-molecular bond distances and angles (Table S4), anisotropic full displacement parameters (Table S5), hydrogen atoms positions (Tables S6) and H-bond distances and angles (Table S7) are available from the authors upon request. A CIF file with details of the crystal structure reported in the paper has been deposited with the Cambridge Crystallographic Data Centre (12 Union Road, Cambridge CB2 1EZ, UK; fax: +44-1223/336-033; Email: deposit@ccdc.cam.ac.uk) and can be obtained free of charge at www.ccdc.cam.ac.uk/conts/retrieving.html, reference number CCDC 874914.

References

[1] D. Rehder, Future Med. Chem. 4 (2012) 1823–1837.
[2] D. Rehder, Bioinorganic Vanadium Chemistry, John Wiley & Sons, Chichester, 2008.
[3] K.H. Thompson, J. Lichter, C. LeBel, M.C. Scaife, J.H. McNeil, C. Orvig, J. Inorg. Biochem. 103 (2009) 554–558.
[4] K.H. Thompson, C. Orvig, J. Chem. Soc. Dalton Trans. (2000) 2885–2892.
[5] H. Sakurai, Y. Kojima, Y. Yoshikawa, K. Kawabe, H. Yasui, Coord. Chem. Rev. 226 (2002) 187–198.
[6] T. Kiss, T. Jakusch, D. Hollender, A. Dornyei, E.A. Enyedy, J. Costa Pessoa, H. Sakurai, A. Sanz-Medel, Coord. Chem. Rev. 252 (2008) 1153–1162.
[7] G.R. Willsky, L.H. Chi, M. Godzala, P.J. Kostyniak, J.J. Smee, A.M. Trujillo, J.A. Alfano, W.J. Ding, Z.H. Hu, D.C. Crans, Coord. Chem. Rev. 255 (2011) 2258–2269.
[8] T. Jakusch, J. Costa Pessoa, T. Kiss, Coord. Chem. Rev. 255 (2011) 2218–2226.
[9] A.M. Evangelou, Crit. Rev. Oncol. Hematol. 42 (2002) 249–265.
[10] D. Gambino, Coord. Chem. Rev. 255 (2011) 2193–2203.
[11] D. Gambino, in: M. Aureliano Alves (Ed.), Book of Reviews on Vanadium Biochemistry, Research Signpost, Kerala, India, 2008, p. 285.
[12] R.A. Sánchez-Delgado, A. Anzellotti, Mini-Rev. Med. Chem. 1 (2004) 23–30.
[13] R.A. Sánchez-Delgado, A. Anzellotti, L. Suárez, Metal ions in biological systems, in: H. Sigel, A. Sigel (Eds.), 41: Metal Ions and their Complexes in Medication, Marcel Dekker, New York, 2004, pp. 379–419.
[14] H. Cerecetto, M. González, Pharmaceuticals 3 (2010) 810–838.
[15] D.R. Magalhães Moreira, A.C. Lima Leite, R. Ribeiro dos Santos, M.B.P. Soares, Curr. Drug Targets 10 (2009) 212–231.
[16] A. Cavalli, M.L. Bolognesi, J. Med. Chem. 52 (2009) 7339–7359.
[17] S.P. Fricker, R.M. Mosi, B.R. Cameron, I. Baird, Y. Zhu, V. Anastassov, J. Cox, P.S. Doyle, E. Hansell, G. Lau, J. Langille, M. Olsen, L. Qin, R. Skerlj, R.S.Y. Wong, Z. Santucci, J.H. McKerrow, J. Inorg. Biochem. 102 (2008) 1839–1845.
[18] D. Gambino, L. Otero, Inorg. Chim. Acta 393 (2012) 103–114.
[19] M. Navarro, G. Gabbiani, L. Messori, D. Gambino, Drug Discov. Today 15 (2010) 1070–1077.
[20] A. Martínez, T. Carreon, E. Iniguez, A. Anzellotti, A. Sánchez, M. TYan, A. Sattler, L. Herrera, R.A. Maldonado, R.A. Sánchez-Delgado, J. Med. Chem. 55 (2012) 3867–3877.
[21] F. Dubar, J. Khalife, J. Brocard, D. Dive, C. Biot, Molecules 13 (2008) 2900–2907.
[22] D. Dive, C. Biot, ChemMedChem 3 (2008) 383–391.
[23] C. Biot, D. Dive, Top. Organomet. Chem. 32 (2010) 155–193.
[24] C. Biot, Curr. Med. Chem. Anti-Infective Agents 3 (2004) 135–147.
[25] V. Delespaux, H.P. de Koning, Drug Resist. Updates 10 (2007) 30–50.
[26] I. Ribeiro, A.M. Sevcsik, F. Alves, G. Diap, R. Don, M.O. Harhay, S. Chang, B. Pecoul, PLoS Negl. Trop. Dis. 3 (2009) e484, http://dx.doi.org/10.1371/journal.pntd.0000484.
[27] J.A. Urbina, Drugs Future 35 (2010) 409–420.
[28] P.J. Hotez, D.H. Molyneux, A. Fenwick, J. Kumaresan, S. Ehrlich Sachs, J.D. Sachs, L. Savioli, N. Engl. J. Med. 357 (2007) 1018–1027.
[29] J.D. Maya, B.K. Cassels, P. Iturriaga-Vásquez, J. Ferreira, M. Faúndez, N. Galanti, A. Ferreira, A. Morello, Comp. Biochem. Physiol. A 146 (2007) 601–620.
[30] K. Nussbaum, J. Honek, C.M.C.v.C. Cadmus, T. Efferth, Curr. Med. Chem. 17 (2010) 1594–1617.
[31] S. Croft, M. Barret, J. Urbina, Trends Parasitol. 21 (2005) 508–512.
[32] K. Kinnamon, E.A. Steck, E.S. Rane, Antimicrob. Agents Chemother. 15 (1979) 157–160.

Please cite this article as: M. Fernández, et al., Oxidovanadium(IV) and dioxidovanadium(V) complexes of tridentate salicylaldehyde semicarbazones: Searching for prospective antitry..., J. Inorg. Biochem. (2013), http://dx.doi.org/10.1016/j.jinorgbio.2013.02.010

ARTICLE IN PRESS

[33] J. Benítez, L. Guggeri, I. Tomaz, G. Arrambide, M. Navarro, J. Costa Pessoa, B. Garat, D. Gambino, J. Inorg. Biochem. 103 (2009) 609–616.
[34] J. Benítez, L. Guggeri, I. Tomaz, J. Costa Pessoa, V. Moreno, J. Lorenzo, F.X. Avilés, B. Garat, D. Gambino, J. Inorg. Biochem. 103 (2009) 1386–1394.
[35] J. Benítez, L. Becco, I. Correia, S. Milena Leal, H. Guiset, J. Costa Pessoa, J. Lorenzo, S. Tanco, P. Escobar, V. Moreno, B. Garat, D. Gambino, J. Inorg. Biochem. 105 (2011) 303–311.
[36] P. Noblía, E.J. Baran, L. Otero, P. Draper, H. Cerecetto, M. González, O.E. Piro, E.E. Castellano, T. Inohara, Y. Adachi, H. Sakurai, D. Gambino, Eur. J. Inorg. Chem. (2004) 322–328.
[37] P. Noblía, M. Vieites, P. Parajón-Costa, E.J. Baran, H. Cerecetto, P. Draper, M. González, O.E. Piro, E.E. Castellano, A. Azqueta, A. López, A. Monge-Vega, D. Gambino, J. Inorg. Biochem. 99 (2005) 443–451.
[38] J. Rivadeneira, D. Barrio, G. Arrambide, D. Gambino, L. Bruzzone, S. Etcheverry, J. Inorg. Biochem. 103 (2009) 633–642.
[39] D. Gambino, M. Fernández, D. Santos, G.A. Etcheverría, O.E. Piro, F.R. Pavan, C.Q.F. Leite, I. Tomaz, F. Marques, Polyhedron 30 (2011) 1360–1366.
[40] W.J. Geary, Coord. Chem. Rev. 7 (1971) 81–91.
[41] A. Rockenbauer, L. Korecz, Appl. Magn. Reson. 10 (1996) 29–43.
[42] N.D. Chasteen, in: J. Lawrence, L. Berliner, J. Reuben (Eds.), Biological Magnetic Resonance, 3, Plenum Press, New York, 1981, pp. 53–119.
[43] L. Casella, M. Gullotti, A. Pintar, S. Colonna, A. Manfredi, Inorg. Chim. Acta 144 (1988) 89–97.
[44] CrysAlisPro, Oxford Diffraction Ltd., Version 1.171.33.48 (release 15–09–2009 CrysAlis171.NET), 2009.
[45] G.M. Sheldrick, SHELXS-97, Program for Crystal Structure Resolution, Univ. of Göttingen, Göttingen, Germany, 1997.
[46] G.M. Sheldrick, SHELXL-97, Program for Crystal Structures Analysis, Univ. of Göttingen, Göttingen, Germany, 1997.
[47] B. Demoro, C. Sarniguet, R. Sánchez-Delgado, M. Rossi, D. Liebowitz, F. Caruso, C. Olea-Azar, V. Moreno, A. Medeiros, M.A. Comini, L. Otero, D. Gambino, Dalton Trans. 41 (2012) 1534–1543.
[48] H. Hirumi, K. Hirumi, J. Parasitol. 75 (1989) 985–989.
[49] C. Hansch, A. Leo, The hydrophobic parameter: measurement and calculation, Exploring QSAR, Fundamentals and Applications in Chemistry and Biology, American Chemical Society Ed, Washington, 1995, pp. 97–124.
[50] A. Tsantili-Kakoulidou, A. Antoniadou-Vyza, Prog. Clin. Biol. Res. 291 (1989) 71–74.
[51] W.A. Denny, J.A. Graham, P.B. Roberts, R.F. Anderson, M. Boyd, C.J.L. Lock, W.R. Wilson, J. Med. Chem. 35 (1992) 4832–4841.
[52] H. Cerecetto, R. Di Maio, M. González, M. Risso, P. Saenz, G. Seoane, A. Denicola, G. Peluffo, C. Quijano, C. Olea-Azar, J. Med. Chem. 42 (1999) 1941–1950.
[53] C. Urquiola, M. Vieites, G. Aguirre, A. Marín, B. Solano, G. Arrambide, M.L. Lavaggi, M.H. Torre, M. González, A. Monge, D. Gambino, H. Cerecetto, Bioorg. Med. Chem. 14 (2006) 5503–5509.
[54] M. Vieites, P. Buccino, L. Otero, M. González, O.E. Piro, R. Sánchez-Delgado, C.M. Sant'Anna, E. Barreiro, H. Cerecetto, D. Gambino, Inorg. Chim. Acta 358 (2005) 3065–3074.
[55] S. Nica, M. Rudolph, H. Gorls, W. Plass, Inorg. Chim. Acta 360 (2007) 1743–1752.
[56] T. Ghosh, B. Mondal, M. Sutradhar, G. Mukherjee, M.G.B. Drew, Inorg. Chim. Acta 360 (2007) 1753–1761.
[57] C.K. Johnson, ORTEP-II, A Fortran Thermal-Ellipsoid Plot Program, Report ORNL-5318, Oak Ridge National Laboratory, Tennessee, USA, 1976.
[58] T.S. Smith II, R. LoBrutto, V.L. Pecoraro, Coord. Chem. Rev. 228 (2002) 1–18.
[59] K. Wuthrich, Helv. Chim. Acta 48 (1965) 1012–1017.
[60] J. Costa Pessoa, I. Cavaco, I. Correia, I. Tomaz, M.T. Duarte, R.D. Gillard, R.T. Henriques, F.J. Higes, C. Madeira, Inorg. Chim. Acta 293 (1999) 1–11.
[61] J. Costa Pessoa, I. Cavaco, I. Correia, D. Costa, R.T. Henriques, R.D. Gillard, Inorg. Chim. Acta 305 (2000) 7–13.
[62] G. Micera, V.L. Pecoraro, E. Garribba, Inorg. Chem. 48 (2009) 5790–5796.
[63] J. Costa Pessoa, M.J. Calhorda, I. Cavaco, I. Correia, M.T. Duarte, V. Felix, R.T. Henriques, M.F.M. Piedade, I. Tomaz, J. Chem. Soc. Dalton Trans. (2002) 4407–4415.
[64] M.R. Maurya, A.A. Khan, A. Azam, S. Ranjan, N. Mondal, A. Kumar, F. Avecilla, J. Costa Pessoa, Dalton Trans. 39 (2010) 1345–1360.
[65] E.H. Kerns, L. Di, Drug-like Properties: Concepts, Structure Design and Methods from ADME to Toxicity Optimization, Academic Press, Amsterdam, 2008.
[66] H. Kubinyi, Arzneim.-Forsch. 26 (1976) 1991–1997.
[67] G.B. Onoa, G. Cervantes, V. Moreno, M.J. Prieto, Nucleic Acids Res. 26 (1998) 1473–1480.
[68] M. Vieites, P. Smircich, M. Pagano, L. Otero, F. Luane Fischer, H. Terenzi, M.J. Prieto, V. Moreno, B. Garat, D. Gambino, J. Inorg. Biochem. 105 (2011) 1704–1711.

Please cite this article as: M. Fernández, et al., Oxidovanadium(IV) and dioxidovanadium(V) complexes of tridentate salicylaldehyde semicarbazones: Searching for prospective antitry..., J. Inorg. Biochem. (2013), http://dx.doi.org/10.1016/j.jinorgbio.2013.02.010